THE JOURNAL OF PHYSICAL CHEMISTRY Letters

pubs.acs.org/JPCL Letter

Accurate and Numerically Efficient r^{2}SCAN Meta-Generalized Gradient Approximation

James W. Furness,* Aaron D. Kaplan, Jinliang Ning, John P. Perdew, and Jianwei Sun*

Cite This: *J. Phys. Chem. Lett.* 2020, 11, 8208–8215 Read Online

ACCESS | Metrics & More | Article Recommendations | Supporting Information

ABSTRACT: The recently proposed rSCAN functional [*J. Chem. Phys.* 2019 *150*, 161101] is a regularized form of the SCAN functional [*Phys. Rev. Lett.* 2015 *115*, 036402] that improves SCAN's numerical performance at the expense of breaking constraints known from the exact exchange–correlation functional. We construct a new meta-generalized gradient approximation by restoring exact constraint adherence to rSCAN. The resulting functional maintains rSCAN's numerical performance while restoring the transferable accuracy of SCAN.

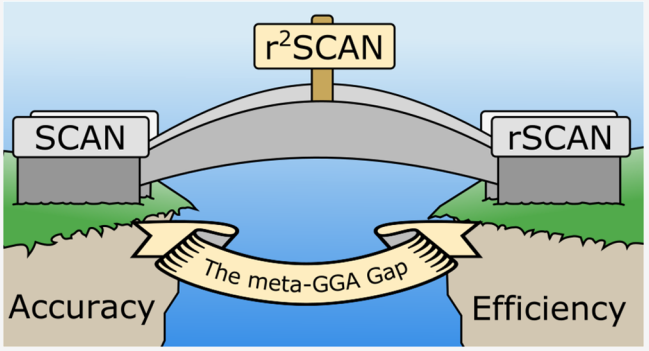

There is a fundamental trade-off at the heart of all large-scale chemical and material computational studies between prediction accuracy and computational efficiency. The level of theory used must simultaneously make accurate and efficient material property predictions. For many projects, Kohn–Sham density functional theory (KS-DFT) presents an appealing compromise, delivering useful accuracy and favorable algorithmic complexity.

The Materials Project database presents a case study of finding such a balance,[1] stating an ambitious mission of "removing the guesswork from materials design by computing properties of all known materials".[2] At the time of writing, the database lists 125 000 inorganic structures calculated from KS-DFT using the Perdew–Burke–Ernzerhof (PBE) generalized gradient approximation (GGA) exchange–correlation (XC) functional.[3] While GGA functionals can be impressively accurate for many properties, they cannot be systemically accurate for all properties,[4−6] and the last 10 years have shown that meta-GGA functionals can improve predictions for similar computational cost.

Meta-GGAs are commonly designed around constraints known for the exact XC functional while minimizing the number of free parameters that must be fit. Functionals derived in this way are termed "non-empirical," and we refer the reader to the Supporting Information of ref 7 for precise definitions of all the exact constraints known for meta-GGAs. Alternatively, the functional can be built from a more flexible form that allows some exact constraints to be broken, so that free parameters can be tuned for accuracy to reference data sets. Functionals taking the latter route, termed "empirical" functionals, tend to be less reliable for systems outside their fitting sets, making a non-empirical functional desirable for large-scale applications.

The strongly constrained and appropriately normed (SCAN) functional[7] recovers all 17 exact constraints presently known for meta-GGA functionals and has shown good transferable accuracy, even for systems challenging for DFT methods. Examples include predicting accurate geometries and energetics for diverse ice and silicon phases[8] and for polymorphs of MnO_2.[9] SCAN accurately reproduces the complex doping-driven metal–insulator transition, magnetic structure, and charge-spin stripe phases of cuprate[10−12] high-temperature superconductors and iridates.[13] It is one of the few functionals that predicts ice as less dense than liquid water under standard conditions,[14] and its description of intermediate range van der Waals interactions has been used to study the dynamics of liquid water.[14,15] Combination of SCAN with beyond DFT techniques such as van der Waals functionals and the Hubbard *U* self-interaction correction have proven effective for modeling the ionic and electronic structures of transition metal oxides.[16−18]

Despite these successes, SCAN's utility for large-scale projects is limited by its sensitivity to the density of the numerical integration grid used during calculation. This poor numerical performance in many codes mandates the use of

Received: August 6, 2020
Accepted: September 2, 2020
Published: September 2, 2020

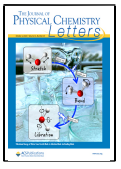

https://dx.doi.org/10.1021/acs.jpclett.0c02405
J. Phys. Chem. Lett. 2020, 11, 8208–8215

dense integration grids which reduces SCAN's computational efficiency,[19,20] and divergence in the associated XC potential has hindered the generation of SCAN pseudopotentials.[21,22] Neither limitation is inherent to the meta-GGA level or SCAN-like functionals, as we will show.

Some modifications to SCAN have been proposed to improve its accuracy for specific systems. The revSCAN functional is a simple modification to the slowly varying limit of SCAN's correlation energy to eliminate the fourth-order term in SCAN's correlation energy density-gradient expansion.[23] The TASK functional is a complete revision of SCAN designed to accurately predict band gaps while retaining the exact constraints placed on the exchange energy,[24] though TASK uses a local spin-density approximation (LSDA) to model correlation. It is not expected that these modifications address the numerical inefficiencies of the parent functional.

In recent work, Bartók and Yates propose a regularized SCAN termed "rSCAN" that aims to control SCAN's numerical challenges while changing as little as possible from the parent functional.[22] The resulting functional shows greatly improved numerical stability and enables pseudopotential generation. While initial testing suggested that rSCAN maintained the accuracy and transferability of SCAN, expanded testing by Mejía-Rodríguez and Trickey[25,26] shows that some transferability is lost, with accuracy for atomization energies[27] particularly degraded.

The need for a computationally efficient revision of SCAN is made plain in Figure 1. This figure shows three meta-GGAs:

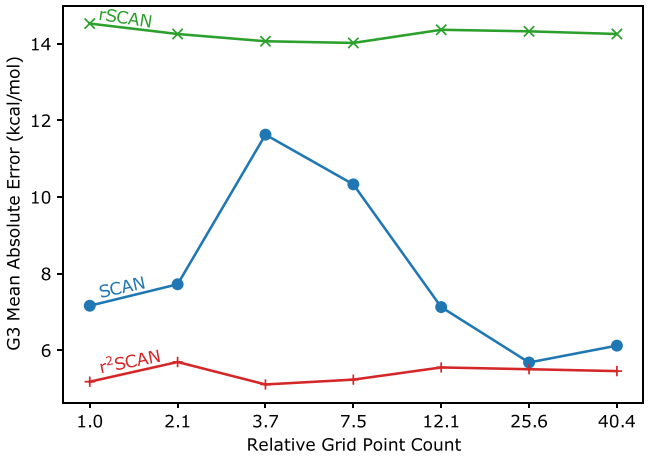

Figure 1. Mean absolute error (MAE) of atomization energies (kcal/mol) for the G3 set of 226 molecules[28] as a function of increasing numerical integration grid density expressed relative to the smallest grid. The grids were chosen from TURBOMOLE[29,30] grid levels 1−7.

SCAN and rSCAN, which have already been introduced, and a novel meta-GGA, r^{2}SCAN, that is the topic of this Letter. It illustrates a grid problem that arises for SCAN in codes with localized basis functions. The horizontal axis shows increasing integration grid density, and the vertical axis shows the mean absolute error (MAE) of the G3 test set[28] of 226 atomization energies. It would be difficult to assert that any of the grid settings present a converged SCAN energy, with SCAN errors varying unpredictably by a factor of 2. While rSCAN stabilizes SCAN numerically, its error offers little improvement over GGAs (e.g., PBE has a MAE of 22.2 kcal/mol[7] for the G3 set). The need for a meta-GGA that retains the accuracy of SCAN, with the grid efficiency of rSCAN, is evident. No such grid problem is found for SCAN in the plane-wave code VASP, as shown in the Supporting Information. However, in VASP, r^{2}SCAN seems to converge with fewer iterations than SCAN does.

The SCAN functional is constructed using a dimensionless kinetic energy variable

$$\alpha(\mathbf{r}) = \frac{\tau(\mathbf{r}) - \tau_{\mathrm{W}}(\mathbf{r})}{\tau_{\mathrm{unif}}(\mathbf{r})} \tag{1}$$

where $\tau = \sum_i |\nabla\phi_i|^2\Theta(\mu - \varepsilon_i)/2$ is the positive kinetic energy density; $\phi_i(\mathbf{r})$ are the Kohn−Sham orbitals; $\Theta(\mu - \varepsilon_i)$ is the orbital occupation; $\tau_{\mathrm{W}} = |\nabla n|^2/(8n)$ is the von Weizsäcker kinetic energy density; $\tau_{\mathrm{unif}} = 3(3\pi^2)^{2/3}n^{5/3}/10$ is the kinetic energy density of a uniform electron gas; μ is the chemical potential; and ε_i are the orbital energies. SCAN uses α to tune functional performance for the local chemical environment.[31] While α allows SCAN to satisfy exact constraints that would be contradictory at the GGA level,[32] α can introduce numerical sensitivity and divergences in the XC potential.[33,34]

The design of rSCAN prioritizes numerical efficiency over satisfaction of exact constraints and instead uses a regularized α'

$$\tilde{\alpha}(\mathbf{r}) = \frac{\tau(\mathbf{r}) - \tau_{\mathrm{W}}(\mathbf{r})}{\tau_{\mathrm{unif}}(\mathbf{r}) + \tau_{\mathrm{r}}} \tag{2}$$

$$\alpha'(\mathbf{r}) = \frac{\tilde{\alpha}(\mathbf{r})^3}{\tilde{\alpha}(\mathbf{r})^2 + \alpha_{\mathrm{r}}} \tag{3}$$

where $\tau_{\mathrm{r}} = 10^{-4}$ and $\alpha_{\mathrm{r}} = 10^{-3}$ are regularization constants. While the choice of a constant τ_{r} eliminates numerical instability as $\alpha \to 0$, α' does not retain the correct uniform and nonuniform scaling properties of α, nor the correct uniform density limit.

For a uniform electron gas, $\alpha \to 1$, which SCAN uses to recover the LSDA exactly. In rSCAN, $\tilde{\alpha} \to 1/(1 + \tau_{\mathrm{r}}/\tau_{\mathrm{unif}})$ which varies with the density, losing the correct uniform electron gas description. It has been shown that recovery of the uniform gas limit is critical for an accurate description of solids, atoms, and molecules.[35,36]

For a slowly varying electron gas, the exchange and correlation energies have well-known expansions in powers of the gradient of the density. Let $s = |\nabla n|/(2k_{\mathrm{F}}n)$, a dimensionless density-gradient on the scale of the Fermi wavevector $k_{\mathrm{F}} = (3\pi^2 n)^{1/3}$, and $q = \nabla^2 n/(4k_{\mathrm{F}}{}^2 n)$ a dimensionless density-Laplacian. The gradient expansion for the exchange energy per particle $\varepsilon_{\mathrm{x}}(\mathbf{r})$ is[37]

$$\varepsilon_{\mathrm{x}} = \varepsilon_{\mathrm{x}}^{\mathrm{LDA}}\left[1 + \mu_{\mathrm{AK}}p + \frac{146}{2025}\left(q^2 - \frac{5}{2}pq\right)\right] + O[(\nabla n)^6] \tag{4}$$

where $\varepsilon_{\mathrm{x}}^{\mathrm{LDA}} = -3k_{\mathrm{F}}/(4\pi)$, $p = s^2$, and $\mu_{\mathrm{AK}} = 10/81$. For the correlation energy, following ref 3, we define an additional dimensionless density-gradient $t = |\nabla n|/[2k_{\mathrm{s}}\phi(\zeta)n]$ on the scale of the Thomas-Fermi screening wavevector $k_{\mathrm{s}} = \sqrt{4k_{\mathrm{F}}/\pi}$. Here $\phi(\zeta) = [(1 + \zeta)^{2/3} + (1 - \zeta)^{2/3}]/2$ is a spin-scaling function of the spin-polarization $\zeta = (n_\uparrow - n_\downarrow)/n$. Then the density-gradient expansion of the correlation energy per particle $\varepsilon_{\mathrm{c}}(\mathbf{r})$ is[3,7,38]

$$\varepsilon_{\mathrm{c}} = \varepsilon_{\mathrm{c}}^{\mathrm{LSDA}} + \phi(\zeta)^3\beta(r_{\mathrm{s}})t^2 \tag{5}$$

https://dx.doi.org/10.1021/acs.jpclett.0c02405
J. Phys. Chem. Lett. 2020, 11, 8208−8215

where $\beta(r_s)$ is a weakly varying function of the Wigner−Seitz radius $r_s = (4\pi n/3)^{-1/3}$, with a maximum $\beta(0) \approx 0.066725$. The kinetic energy density τ has an analogous but unwieldy density-gradient expansion.[39] It is generally understood that recovering the exact density-gradient expansion is relevant for solids.[40] These terms also affect the asymptotic behavior of E_{xc} for atoms,[41] as the asymptotic limit for atoms of large-Z is a semiclassical limit that is described exactly by the LSDA at lowest-order, with the density-gradient terms modulating the higher-order terms (known accurately).[41] Thus, the uniform and slowly varying density limits are relevant to both solid-state and atomic systems.

SCAN eliminates erroneous contributions from α to the second- and fourth-order slowly varying density-gradient expansion (GE2 and GE4, respectively) of E_{xc} by using a nonanalytic switching function whose value and derivatives of all orders are zero at $\alpha = 1$. While theoretically convenient, constraining the interpolation function to have zero derivatives at $\alpha = 1$ results in a twisted function that harms numerical performance. The SCAN interpolation function was replaced with a smooth polynomial in rSCAN (see Figure 2) to remove this source of numeric instability, at the expense of introducing second- and fourth-order contributions from α to the density-gradient expansion of E_{xc}.

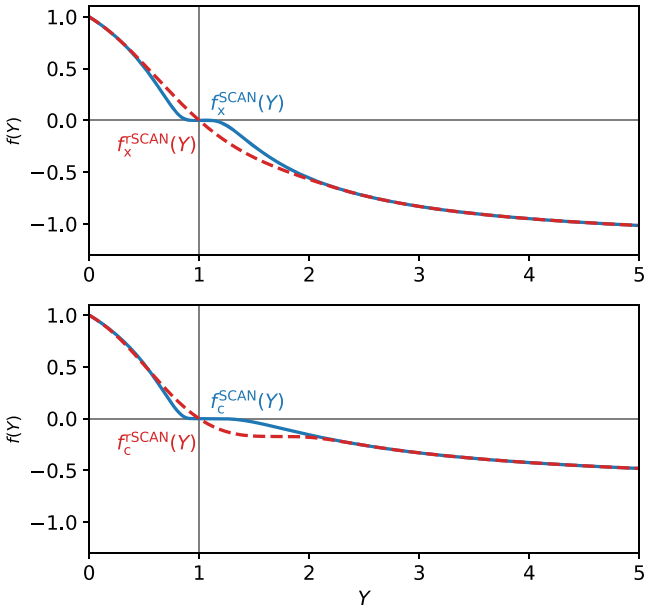

Figure 2. SCAN (blue, solid) and rSCAN (red, dashed) interpolation functions plotted for a generic stand-in iso-orbital indicator "Y" (α for SCAN, α' for rSCAN, $\bar{\alpha}$ for r^{2}SCAN). The functions mix $Y = 0$ (single orbital) and $Y = 1$ (uniform density limit for α and $\bar{\alpha}$) energy densities. The derivatives of the SCAN interpolation functions vanish to all orders in Y at $Y \to 1$, allowing SCAN to recover the appropriate density-gradient expansions exactly in the slowly varying limit. The rSCAN interpolation functions are used with $Y = \bar{\alpha}$ in r^{2}SCAN, and their smooth, nonvanishing first derivatives at $Y = 1$ necessitate changes from SCAN to r^{2}SCAN in the $Y = 1$ energy densities.

It is clear then that rSCAN makes wide-ranging sacrifices in exact constraint adherence in order to make a numerically efficient meta-GGA. Here, we will show definitively that such sacrifices are needless and derive revisions to the rSCAN functional to restore exact constraint adherence without harming numerical efficiency. We apply these revisions to build a regularized−restored SCAN functional, r^{2}SCAN, which recovers the most important exact constraints of SCAN. Table 1 summarizes the constraint satisfaction of the functionals

Table 1. Summary of Exact Constraint Adherence for a Subset of the 17 Known Exact Constraints Applicable to Meta-GGA Functionals[a]

	SCAN	rSCAN	r^{2}SCAN
uniform density	√	–	√
coordinate scaling	√	–	√
GE2	√	–	√
GE4X	√	–	–

[a]Here, GE2 denotes the second-order slowly-varying density-gradient expansion, and GE4X denotes the fourth-order GE for exchange.

concerned, and we stress that because only appropriate norm systems[7] were used to set the free parameters, all three functionals (SCAN, rSCAN, and r^{2}SCAN) may be considered non-empirical. For brevity, we show only parts of the functional that are modified in this work and direct the reader to Section S2 of the Supporting Information for a full definition of the relevant equations.

There are many situations where the exact exchange−correlation potential and energy density can be expected to be reasonably smooth (see, e.g., the plots of highly accurate exchange−correlation potentials and energy densities of simple hydrides in ref 42). In general, the exact Kohn−Sham exchange−correlation potential need not be smooth, as demonstrated by the Perdew−Parr−Levy−Balduz theorem:[43] the exchange−correlation potential, as a function of the number of electrons N, exhibits discontinuities across integer values of N, with steps and peaks in the low-density region between two separated dissimilar systems. However, a semilocal functional cannot recover the precise behaviors of the exact exchange−correlation energy and potential and instead averages over them. Therefore, we consider smoothness of the energy density and potential to be a necessary construction principle of semilocal approximate density functionals. A construction principle is any physically or mathematically motivated principle that can supplement the design of a first-principles density functional approximation.

The correct uniform- and nonuniform-scaling properties of α, as well as the correct uniform density limit of E_{xc}, are recovered in r^{2}SCAN by regularizing α as

$$\bar{\alpha} = \frac{\tau - \tau_W}{\tau_{unif} + \eta\tau_W} \tag{6}$$

where $\eta = 10^{-3}$ is a simple regularization parameter. Note that because $\tau \geq \tau_W$, $\bar{\alpha}$ has the same range as α, $0 \leq \bar{\alpha} < \infty$. This is distinct from the dimensionless kinetic energy variable suggested by ref 34

$$\beta = \frac{\tau - \tau_W}{\tau + \tau_{unif}} \tag{7}$$

which ranges between $0 \leq \beta < 1$ and has less rapidly varying derivatives than α. As this work seeks revisions to SCAN, we will not consider β or related iso-orbital indicators here and adopt $\bar{\alpha}$ as the iso-orbital indicator used throughout r^{2}SCAN.

SCAN uses the iso-orbital indicator variable α to drive interpolation functions $f_{x/c}(\alpha)$ for exchange and correlation. The rSCAN functional replaces the original SCAN interpolation functions with a polynomial function of α' when $\alpha' <$

https://dx.doi.org/10.1021/acs.jpclett.0c02405
J. Phys. Chem. Lett. 2020, 11, 8208−8215

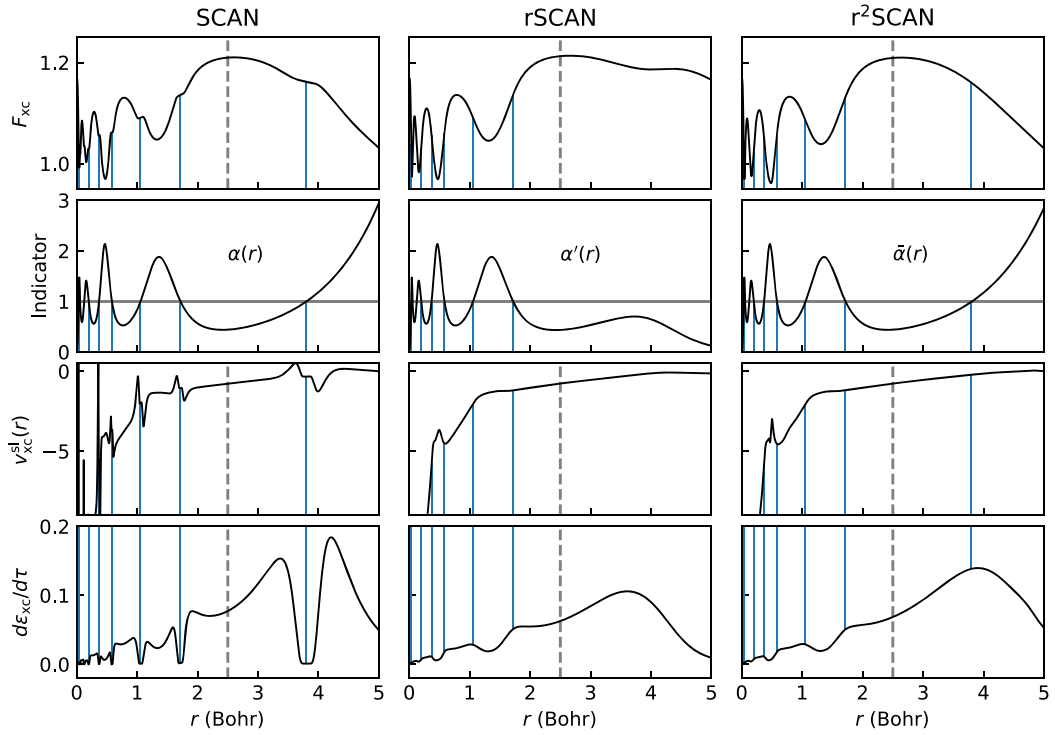

Figure 3. (Top) Exchange−correlation enhancement factors; (middle-upper) iso-orbital indicator $\alpha(r)$, $\alpha'(r)$, or $\bar{\alpha}$ (r) as appropriate; (middle-lower) semilocal part of the exchange−correlation potential as in eq 11; and (bottom) derivative of exchange−correlation energy density with respect to kinetic energy density. Calculated for the xenon atom from accurate Hartree−Fock Slater orbitals[48] for the SCAN,[7] rSCAN,[22] and r²SCAN functionals. The VASP[49−52] projector-augmented wave[53] pseudopotential cutoff radius (2.5 Bohr) is illustrated by a dashed vertical line. Solid vertical lines show where $\alpha = 1$.

2.5 that smooths out the plateau-like behavior of the original near $\alpha = 1$. The r²SCAN functional adopts the rSCAN interpolation function but uses $\bar{\alpha}$ as the indicator variable. Both the SCAN and rSCAN interpolation functions are shown in Figure 2 as functions of a generic indicator.

The SCAN interpolation function was designed to have vanishing derivatives at $\alpha = 1$, but the rSCAN replacements go linearly through zero at this point. As a result of these nonvanishing derivatives, the interpolation function makes spurious contributions to the slowly varying density-gradient expansions that break the corresponding exact constraints. The r²SCAN functional recovers the gradient expansions through $O[(\nabla n)^2]$ while using the rSCAN polynomial interpolation by directly canceling spurious terms in the slowly varying energy densities.

For exchange we recover the gradient expansion by replacing the $x(p, \alpha')$ function of SCAN and rSCAN with

$$x(p) = \{C_\eta C_{2x} \exp[-p^2/{d_{p2}}^4] + \mu_{AK}\}p \tag{8}$$

Here, the constants $C_\eta = 20/27 + 5\eta/3$, depending on the $\bar{\alpha}$ regularization parameter $\eta = 10^{-3}$, and $C_{2x} \approx -0.162742$ eliminate erroneous contributions from $df_x(\bar{\alpha})/d\bar{\alpha}$ at $\bar{\alpha} \to 1$, and $d_{p2} = 0.316$ is a damping parameter determined as the maximal value (therefore least damped) required to recover SCAN's error for the rare gas atom and jellium surface appropriate norms described in ref 7. Replacing α' with $\bar{\alpha}$ and $x(p, \alpha')$ with eq 8 in the rSCAN functional defines r²SCAN exchange and restores the uniform density limit, correct scaling properties, and GE2 for exchange (GE2X). As in ref 7 and earlier work, we employ the exact spin-scaling equality for the exchange energy;[44] thus, only formulas for spin-unpolarized exchange need to be displayed.

From eq 4, we see that a meta-GGA recovering GE4X must either explicitly include the Laplacian of the density as an ingredient or recover q-dependent terms via integration by parts on τ. The latter method, used in SCAN, is theoretically sound but likely introduces further numerical instabilities due to an increased sensitivity to α. Furthermore, the gradient expansion for the correlation energy is known only to second order, and the relevance of GE4X (beyond GE2X terms) to real systems has not been established. To ensure that our functional is numerically stable we consider only GE2X here and defer further discussion of GE4X and its difficulties to a further publication in the near future.

The gradient expansion for correlation is known only to second order, and we recover it by replacing the $g(At^2)$ function which appears in the slowly varying correlation energy density of rSCAN and SCAN with

$$g(At^2, \Delta y) = [1 + 4(At^2 - \Delta y)]^{-1/4} \tag{9}$$

$$\Delta y = \frac{\Delta f_{c2}}{27\gamma d_s \phi^3 w_1}\left\{20 r_s\left[\frac{\partial \varepsilon_c^{LSDA0}}{\partial r_s} - \frac{\partial \varepsilon_c^{LSDA1}}{\partial r_s}\right] - 45\eta[\varepsilon_c^{LSDA0} - \varepsilon_c^{LSDA1}]\right\} p \exp[-p^2/d_{p2}^4] \tag{10}$$

Here Δy is the new term introduced in r²SCAN that eliminates erroneous contributions from $df_c(\bar{\alpha})/d\bar{\alpha}$ at $\bar{\alpha} \to 1$. Replacing α' with $\bar{\alpha}$ and $g(At^2)$ with eqs 9 and 10 in rSCAN correlation defines r²SCAN correlation and approximately recovers GE2C.

https://dx.doi.org/10.1021/acs.jpclett.0c02405
J. Phys. Chem. Lett. 2020, 11, 8208−8215

Table 2. Mean Error (ME) and Mean Absolute Error (MAE) of TPSS,[59] SCAN,[7] rSCAN,[22] and r^{2}SCAN for the G3 Set of 226 Molecular Atomization Energies,[28] the BH76 Set of 76 Chemical Barrier Heights,[54] the S22 set of 22 Interaction Energies between Closed Shell Complexes,[55] and the LC20 Set of 20 Solid Lattice Constants[56a]

	G3		BH76		S22		LC20	
	ME	MAE	ME	MAE	ME	MAE	ME	MAE
TPSS	−5.2	5.8	−8.6	8.6	−3.4	3.4	0.033	0.041
SCAN	−5.0	6.1	−7.7	7.7	−0.5	0.8	0.009	0.015
rSCAN	−14.0	14.3	−7.4	7.4	−1.2	1.3	0.020	0.025
r^{2}SCAN	−4.5	5.5	−7.1	7.2	−0.9	1.1	0.022	0.027

[a]Errors for G3, BH76, and S22 sets are in kcal/mol, whereas errors for LC20 are in Å. We did not make corrections for basis set superposition error for the S22 set which used the aug-cc-pVTZ basis set.[60] All calculations for G3 and BH76 used the 6-311++G(3df,3pd) basis set.[28,61] Details of the computational methods are included in Section S1 of the Supporting Information.

In eq 10, $\Delta f_{c2} \approx -0.711402$ and $\gamma = (1 - \ln 2)/\pi^2 \approx 0.031091$ are constants; all other quantities are functions defined in the Supporting Information. The correlation gradient expansion of r^{2}SCAN becomes exact whenever $|\nabla\zeta| = 0$ and approximately recovers GE2C for all other values of $\nabla\zeta$. Thus, r^{2}SCAN recovers GE2C exactly for spin-unpolarized systems, where the correlation energy is likely most negative, and for fully spin-polarized systems, where the correlation energy is likely least negative. Between these limits, the r^{2}SCAN correlation gradient expansion is a reasonable approximation to the true gradient expansion.

These modifications should not degrade the good numerical performance of rSCAN. Their effect can be seen in Figure 3, which compares the XC enhancement factor and XC potential components of SCAN and r^{2}SCAN for the xenon atom. The implicit orbital dependence of τ-dependent meta-GGA functionals prevents direct evaluation of a multiplicative KS potential, and such functionals are more commonly implemented using derivatives with respect to individual orbitals in a generalized Kohn−Sham scheme.[45−47] Let $\epsilon_{xc} = n\varepsilon_{xc}$ be the XC energy density. We can identify a multiplicative component of the potential

$$v_{xc}^{sl}(\mathbf{r}) = \frac{\partial \epsilon_{xc}(\mathbf{r})}{\partial n(\mathbf{r})} - \nabla\cdot\left[\frac{\partial \epsilon_{xc}(\mathbf{r})}{\partial|\nabla n(\mathbf{r})|}\frac{\nabla n(\mathbf{r})}{|\nabla n(\mathbf{r})|}\right] \tag{11}$$

and summarize the nonmultiplicative component as the derivative of the energy density with respect to τ. Both are shown in Figure 3.

While the overall intershell features of the F_{xc} are similar between the two functionals, SCAN shows plateaus where $\alpha = 1$, while r^{2}SCAN is smooth throughout. This behavior is echoed as sharp oscillations in both the multiplicative potential component and nonmultiplicative τ derivative for SCAN, which contrasts with the smooth equivalents for r^{2}SCAN. We suggest that r^{2}SCAN may make generation of meta-GGA pseudopotentials feasible. Note that on the scale of Figure 3 both α and $\bar{\alpha}$ appear to diverge. While it is true that α diverges, the η regularization parameter ensures $\bar{\alpha}$ remains finite, with a final maxima occurring around 8 Bohr after which it asymptotically approaches 0. Larger values of η cause the asymptotic return to occur closer to the nuclei but cause the regularization to have a greater impact on predicted energies. We defer detailed discussion of η and single-orbital system potential divergence to Supporting Information Section S3.

Reference 25 shows that atomization energies are particularly problematic for rSCAN, with its error being roughly twice that of SCAN's. As such, we take the G3 set of 226 atomization energies[28] as a primary means of assessing the effect of constraint restoration. Table 2 summarizes the accuracy of the functionals for the G3 set using the most dense grid available. We find that the error for rSCAN is roughly twice that of SCAN, consistent with other studies. The new r^{2}SCAN functional shows similar accuracy to SCAN, supporting the importance of exact constraint adherence.

We restate that the improved numerical efficiency of r^{2}SCAN is immediately apparent from Figure 1, which shows accuracy for the G3 test set as a function of integration grid density. r^{2}SCAN shows consistent error with grid density, similar to rSCAN and in sharp contrast to SCAN. This figure should stand as a stark warning that studies comparing total energies from SCAN must carefully test for grid convergence and shows the utility of the new regularized−restored functional which achieves consistently good accuracy with even the smallest grids.

The transferablility of the new functionals was further tested for 76 reaction barrier heights,[54] 22 weak interaction energies,[55] and 20 lattice constants,[56] with error statistics summarized in Table 2. All SCAN derived functionals show similar performance across the test sets, with the exception of the G3 atomization energy set as discussed above. The LC20 set was assessed by fitting the stabilized jellium equation of state (SJEOS)[57,58] to single-point energies at a range of lattice volumes around equilibrium.

We recently learned of a "de-orbitalization"[62−64] of our r^{2}SCAN that replaces the exact orbital-dependent Kohn−Sham kinetic energy density τ by a posited function of n, ∇n, and $\nabla^2 n$, called "r^{2}SCAN-L".[65] This speeds up computations while somewhat reducing overall accuracy, though interestingly the accuracy of the magnetic moment of metallic Fe is restored by the deorbitalization to the good level of LSDA and PBE. As a possible explanation, we note that the exact τ has a fully nonlocal dependence upon the electron density n that is needed to satisfy some exact constraints and is probably needed for optimal accuracy in atoms, molecules, and insulators. This full nonlocality may however be somewhat harmful for metals, where metallic screening can favor truly semilocal approximations to the valence−valence exchange−correlation energy.

We have presented r^{2}SCAN as a functional combining SCAN's transferable accuracy from exact constraint satisfaction with rSCAN's numerical efficiency. r^{2}SCAN satisfies the most important exact constraints of SCAN. In our future work, we will assess the importance of the GE4X terms beyond GE2X (recovered by SCAN, but not by r^{2}SCAN) as an exact constraint. We draw this conclusion from the competitive accuracy shown for the diverse test sets of Table 2 and the rapid grid convergence of Figure 1. The XC potential analysis

https://dx.doi.org/10.1021/acs.jpclett.0c02405
J. Phys. Chem. Lett. 2020, 11, 8208−8215

from Figure 3 suggests that r^{2}SCAN will be preferable when a smooth potential is critical. In particular, it should now be more practical to construct a pseudopotential and to evaluate the second functional derivative which can play the role of an exchange−correlation kernel in time-dependent density functional applications. We expect the new regularized−restored SCAN functional to bridge the gap between accuracy and numerical efficiency and enable meta-GGA use in large-scale computational studies.

■ ASSOCIATED CONTENT

Supporting Information

The Supporting Information is available free of charge at https://pubs.acs.org/doi/10.1021/acs.jpclett.0c02405.

Section S1, computational methods and grid convergence in VASP; Section S2, r^{2}SCAN working equations; Section S3, determining η regularization parameter and XC potential divergence; Section S4, reference atomic energies; Section S5, full test set data (PDF)

■ AUTHOR INFORMATION

Corresponding Authors

James W. Furness − *Department of Physics and Engineering Physics, Tulane University, New Orleans, Louisiana 70118, United States;* orcid.org/0000-0003-3146-0977; Email: jfurness@tulane.edu

Jianwei Sun − *Department of Physics and Engineering Physics, Tulane University, New Orleans, Louisiana 70118, United States;* orcid.org/0000-0002-2361-6823; Email: jsun@tulane.edu

Authors

Aaron D. Kaplan − *Department of Physics, Temple University, Philadelphia, Pennsylvania 19122, United States;* orcid.org/0000-0003-3439-4856

Jinliang Ning − *Department of Physics and Engineering Physics, Tulane University, New Orleans, Louisiana 70118, United States;* orcid.org/0000-0002-3691-5291

John P. Perdew − *Department of Physics and Department of Chemistry, Temple University, Philadelphia, Pennsylvania 19122, United States*

Complete contact information is available at: https://pubs.acs.org/10.1021/acs.jpclett.0c02405

Notes

The authors declare no competing financial interest.

■ ACKNOWLEDGMENTS

J.W.F., J.N., and J.S. acknowledge the support of the U.S. DOE, Office of Science, Basic Energy Sciences Grant No. DE-SC0019350 (core research). A.D.K. and J.P.P. acknowledge the support of the U.S. Department of Energy, Office of Science, Basic Energy Sciences, through Grant No. DE-SC0012575 to the Energy Frontier Research Center: Center for Complex Materials from First Principles. We thank Albert Bartók-Partay and Daniel Mejía-Rodríguez for their invaluable discussions around the ideas presented here. J.P.P. thanks Natalie Holzwarth for pointing out that the SCAN exchange−correlation potential for an atom diverges in the tail of the density, making pseudopotential construction difficult. We acknowledge discussions with S. Kümmel.

■ REFERENCES

(1) Jain, A.; Ong, S. P.; Hautier, G.; Chen, W.; Richards, W. D.; Dacek, S.; Cholia, S.; Gunter, D.; Skinner, D.; Ceder, G.; et al. The Materials Project: A materials genome approach to accelerating materials innovation. *APL Mater.* **2013**, *1*, 011002.

(2) Persson, K. *About the Materials Project.* 2020; https://materialsproject.org/about.

(3) Perdew, J. P.; Burke, K.; Ernzerhof, M. Generalized Gradient Approximation Made Simple. *Phys. Rev. Lett.* **1996**, *77*, 3865−3868.

(4) Perdew, J. P.; Ruzsinszky, A.; Csonka, G. I.; Vydrov, O. A.; Scuseria, G. E.; Constantin, L. A.; Zhou, X.; Burke, K. Generalized gradient approximation for solids and their surfaces. *Phys. Rev. Lett.* **2008**, *100*, 136406.

(5) Ruzsinszky, A.; Csonka, G. I.; Scuseria, G. E. Regularized gradient expansion for atoms, molecules, and solids. *J. Chem. Theory Comput.* **2009**, *5*, 763−769.

(6) Tran, F.; Stelzl, J.; Blaha, P. Rungs 1 to 4 of DFT Jacob's ladder: Extensive test on the lattice constant, bulk modulus, and cohesive energy of solids. *J. Chem. Phys.* **2016**, *144*, 204120.

(7) Sun, J.; Ruzsinszky, A.; Perdew, J. P. Strongly Constrained and Appropriately Normed Semilocal Density Functional. *Phys. Rev. Lett.* **2015**, *115*, 036402.

(8) Sun, J.; Remsing, R. C.; Zhang, Y.; Sun, Z.; Ruzsinszky, A.; Peng, H.; Yang, Z.; Paul, A.; Waghmare, U.; Wu, X.; et al. Accurate first-principles structures and energies of diversely bonded systems from an efficient density functional. *Nat. Chem.* **2016**, *8*, 831−836.

(9) Kitchaev, D. A.; Peng, H.; Liu, Y.; Sun, J.; Perdew, J. P.; Ceder, G. Energetics of MnO2 polymorphs in density functional theory. *Phys. Rev. B: Condens. Matter Mater. Phys.* **2016**, *93*, 045132.

(10) Furness, J. W.; Zhang, Y.; Lane, C.; Buda, I. G.; Barbiellini, B.; Markiewicz, R. S.; Bansil, A.; Sun, J. An accurate first-principles treatment of doping-dependent electronic structure of high-temperature cuprate superconductors. *Communications Physics* **2018**, *1*, 1−6.

(11) Lane, C.; Furness, J. W.; Buda, I. G.; Zhang, Y.; Markiewicz, R. S.; Barbiellini, B.; Sun, J.; Bansil, A. Antiferromagnetic ground state of La2CuO4: A parameter-free ab initio description. *Phys. Rev. B: Condens. Matter Mater. Phys.* **2018**, *98*, 125140.

(12) Zhang, Y.; Lane, C.; Furness, J. W.; Barbiellini, B.; Perdew, J. P.; Markiewicz, R. S.; Bansil, A.; Sun, J. Competing stripe and magnetic phases in the cuprates from first principles. *Proc. Natl. Acad. Sci. U. S. A.* **2020**, *117*, 68−72.

(13) Lane, C.; Zhang, Y.; Furness, J. W.; Markiewicz, R. S.; Barbiellini, B.; Sun, J.; Bansil, A. First-principles calculation of spin and orbital contributions to magnetically ordered moments in Sr2IrO4. *Phys. Rev. B: Condens. Matter Mater. Phys.* **2020**, *101*, 155110.

(14) Chen, M.; Ko, H. Y.; Remsing, R. C.; Calegari Andrade, M. F.; Santra, B.; Sun, Z.; Selloni, A.; Car, R.; Klein, M. L.; Perdew, J. P.; et al. Ab initio theory and modeling of water. *Proc. Natl. Acad. Sci. U. S. A.* **2017**, *114*, 10846−10851.

(15) Zheng, L.; Chen, M.; Sun, Z.; Ko, H. Y.; Santra, B.; Dhuvad, P.; Wu, X. Structural, electronic, and dynamical properties of liquid water by ab initio molecular dynamics based on SCAN functional within the canonical ensemble. *J. Chem. Phys.* **2018**, *148*, 164505.

(16) Peng, H.; Perdew, J. P. Synergy of van der Waals and self-interaction corrections in transition metal monoxides. *Phys. Rev. B: Condens. Matter Mater. Phys.* **2017**, *96* (R), 100101.

(17) Sai Gautam, G.; Carter, E. A. Evaluating transition metal oxides within DFT-SCAN and SCAN+U frameworks for solar thermochemical applications. *Physical Review Materials* **2018**, *2*, 095401.

(18) Zhang, Y.; Furness, J. W.; Xiao, B.; Sun, J. Subtlety of TiO2 phase stability: Reliability of the density functional theory predictions and persistence of the self-interaction error. *J. Chem. Phys.* **2019**, *150*, 014105.

(19) Yang, Z.-h.; Peng, H.; Sun, J.; Perdew, J. P. More realistic band gaps from meta-generalized gradient approximations: Only in a generalized Kohn-Sham scheme. *Phys. Rev. B: Condens. Matter Mater. Phys.* **2016**, *93*, 205205.

(20) Yamamoto, Y.; Diaz, C. M.; Basurto, L.; Jackson, K. A.; Baruah, T.; Zope, R. R. Fermi-Löwdin orbital self-interaction correction using the strongly constrained and appropriately normed meta-GGA functional. *J. Chem. Phys.* **2019**, *151*, 154105.
(21) Yao, Y.; Kanai, Y. Plane-wave pseudopotential implementation and performance of SCAN meta-GGA exchange-correlation functional for extended systems. *J. Chem. Phys.* **2017**, *146*, 224105.
(22) Bartók, A. P.; Yates, J. R. Regularized SCAN functional. *J. Chem. Phys.* **2019**, *150*, 161101.
(23) Mezei, P. D.; Csonka, G. I.; Kallay, M. Simple modifications of the SCAN meta-generalized gradient approximation functional. *J. Chem. Theory Comput.* **2018**, *14*, 2469.
(24) Aschebrock, T.; Kümmel, S. Ultranonlocality and accurate band gaps from a meta-generalized gradient approximation. *Physical Review Research* **2019**, *1*, 033082.
(25) Mejía-Rodríguez, D.; Trickey, S. B. Supplementary Material: Comment on "Regularized SCAN functional". *J. Chem. Phys.* **2019**, *151*, 207101.
(26) Bartók, A. P.; Yates, J. R. Response to"Comment on 'Regularized SCAN functional'"[J. Chem. Phys. 151, 207101 (2019)]. *J. Chem. Phys.* **2019**, *151*, 207102.
(27) Yamamoto, Y.; Salcedo, A.; Diaz, C. M.; Alam, M. S.; Baruah, T.; Zope, R. R. Comparison of regularized SCAN functional with SCAN functional with and without self-interaction for a wide-array of properties. *arXiv*, 2020, 2004.13393.
(28) Curtiss, L. A.; Raghavachari, K.; Redfern, P. C.; Pople, J. A. Assessment of Gaussian-3 and density functional theories for a larger experimental test set. *J. Chem. Phys.* **2000**, *112*, 7374−7383.
(29) Treutler, O.; Ahlrichs, R. Efficient molecular numerical integration schemes. *J. Chem. Phys.* **1995**, *102*, 346−354.
(30) Balasubramani, S. G.; Chen, G. P.; Coriani, S.; Diedenhofen, M.; Frank, M. S.; Franzke, Y. J.; Furche, F.; Grotjahn, R.; Harding, M. E.; Hättig, C.; et al. TURBOMOLE: Modular program suite for ab initio quantum-chemical and condensed-matter simulations. *J. Chem. Phys.* **2020**, *152*, 184107.
(31) Sun, J.; Xiao, B.; Fang, Y.; Haunschild, R.; Hao, P.; Ruzsinszky, A.; Csonka, G. I.; Scuseria, G. E.; Perdew, J. P. Density functionals that recognize covalent, metallic, and weak bonds. *Phys. Rev. Lett.* **2013**, *111*, 106401.
(32) Sun, J.; Perdew, J. P.; Ruzsinszky, A. Semilocal density functional obeying a strongly tightened bound for exchange. *Proc. Natl. Acad. Sci. U. S. A.* **2015**, *112*, 685−689.
(33) Holzwarth, N. Private communication, 2018.
(34) Furness, J. W.; Sun, J. Enhancing the efficiency of density functionals with an improved iso-orbital indicator. *Phys. Rev. B: Condens. Matter Mater. Phys.* **2019**, *99*, 041119.
(35) Zope, R. R.; Yamamoto, Y.; Diaz, C. M.; Baruah, T.; Peralta, J. E.; Jackson, K. A.; Santra, B.; Perdew, J. P. A step in the direction of resolving the paradox of Perdew-Zunger self-interaction correction. *J. Chem. Phys.* **2019**, *151*, 214108.
(36) Bhattarai, P.; Wagle, K.; Shahi, C.; Yamamoto, Y.; Romero, S.; Santra, B.; Zope, R. R.; Peralta, J. E.; Jackson, K. A.; Perdew, J. P. A Step in the Direction of Resolving the Paradox of Perdew-Zunger Self-interaction Correction. II. Gauge Consistency of the Energy Density at Three Levels of Approximation. *J. Chem. Phys.* **2020**, *152*, 214109.
(37) Svendsen, P.; von Barth, U. Gradient expansion of the exchange energy from second-order density response theory. *Phys. Rev. B: Condens. Matter Mater. Phys.* **1996**, *54*, 17402−17413.
(38) Ma, S.-K.; Brueckner, K. A. Correlation energy of an electron gas with a slowly varying high density. *Phys. Rev.* **1968**, *165*, 18−31.
(39) Brack, M.; Jennings, B. K.; Chu, Y. H. On the extended Thomas-Fermi approximation to the kinetic energy density. *Phys. Lett. B* **1976**, *65*, 1−4.
(40) Perdew, J. P.; Constantin, L. A.; Sagvolden, E.; Burke, K. Relevance of the slowly varying electron gas to atoms, molecules, and solids. *Phys. Rev. Lett.* **2006**, *97*, 223002.
(41) Elliott, P.; Lee, D.; Cangi, A.; Burke, K. Semiclassical origins of density functionals. *Phys. Rev. Lett.* **2008**, *100*, 256406.
(42) Gritsenko, O. V.; Van Leeuwen, R.; Baerends, E. J. Molecular exchange-correlation Kohn-Sham potential and energy density from ab initio first- and second-order density matrices: Examples for XH (X = Li, B, F). *J. Chem. Phys.* **1996**, *104*, 8535−8545.
(43) Perdew, J. P.; Parr, R. G.; Levy, M.; Balduz, J. L. Density-functional theory for fractional particle number: Derivative discontinuities of the energy. *Phys. Rev. Lett.* **1982**, *49*, 1691−1694.
(44) Oliver, G. L.; Perdew, J. P. Spin-density gradient expansion for the kinetic energy. *Phys. Rev. A: At., Mol., Opt. Phys.* **1979**, *20*, 397−403.
(45) Seidl, A.; Görling, A.; Vogl, P.; Majewski, J.; Levy, M. Generalized Kohn-Sham schemes and the band-gap problem. *Phys. Rev. B: Condens. Matter Mater. Phys.* **1996**, *53*, 3764−3774.
(46) Neumann, R.; Nobes, R. H.; Handy, N. C. Exchange functionals and potentials. *Mol. Phys.* **1996**, *87*, 1−36.
(47) Adamo, C.; Ernzerhof, M.; Scuseria, G. E. The meta-GGA functional: Thermochemistry with a kinetic energy density dependent exchange-correlation functional. *J. Chem. Phys.* **2000**, *112*, 2643−2649.
(48) Clementi, E.; Roetti, C. Roothaan-Hartree-Fock Atomic Wavefunctions. *At. Data Nucl. Data Tables* **1974**, *14*, 177−478.
(49) Kresse, G.; Hafner, J. Ab initio molecular dynamics for liquid metals. *Phys. Rev. B: Condens. Matter Mater. Phys.* **1993**, *47*, 558−561.
(50) Kresse, G.; Hafner, J. Ab initio molecular-dynamics simulation of the liquid-metalamorphous- semiconductor transition in germanium. *Phys. Rev. B: Condens. Matter Mater. Phys.* **1994**, *49*, 14251−14269.
(51) Kresse, G.; Furthmüller, J. Efficient iterative schemes for ab initio total-energy calculations using a plane-wave basis set. *Phys. Rev. B: Condens. Matter Mater. Phys.* **1996**, *54*, 11169−11186.
(52) Kresse, G.; Furthmüller, J. Efficiency of ab-initio total energy calculations for metals and semiconductors using a plane-wave basis set. *Comput. Mater. Sci.* **1996**, *6*, 15−50.
(53) Kresse, G.; Joubert, D. From ultrasoft pseudopotentials to the projector augmented-wave method. *Phys. Rev. B: Condens. Matter Mater. Phys.* **1999**, *59*, 1758−1775.
(54) Zhao, Y.; González-García, N.; Truhlar, D. G. Benchmark database of barrier heights for heavy atom transfer, nucleophilic substitution, association, and unimolecular reactions and its use to test theoretical methods. *J. Phys. Chem. A* **2005**, *109*, 2012−2018.
(55) Jurečka, P.; Šponer, J.; Černý, J.; Hobza, P. Benchmark database of accurate (MP2 and CCSD(T) complete basis set limit) interaction energies of small model complexes, DNA base pairs, and amino acid pairs. *Phys. Chem. Chem. Phys.* **2006**, *8*, 1985−1993.
(56) Sun, J.; Marsman, M.; Csonka, G. I.; Ruzsinszky, A.; Hao, P.; Kim, Y. S.; Kresse, G.; Perdew, J. P. Self-consistent meta-generalized gradient approximation within the projector-augmented-wave method. *Phys. Rev. B: Condens. Matter Mater. Phys.* **2011**, *84*, 035117.
(57) Staroverov, V. N.; Scuseria, G. E.; Tao, J.; Perdew, J. P. Tests of a ladder of density functionals for bulk solids and surfaces. *Phys. Rev. B: Condens. Matter Mater. Phys.* **2004**, *69*, 075102.
(58) Alchagirov, A. B.; Perdew, J. P.; Boettger, J. C.; Albers, R. C.; Fiolhais, C. Energy and pressure versus volume: Equations of state motivated by the stabilized jellium model. *Phys. Rev. B: Condens. Matter Mater. Phys.* **2001**, *63*, 2241151−22411516.
(59) Tao, J.; Perdew, J. P.; Staroverov, V. N.; Scuseria, G. E. Climbing the Density Functional Ladder: Non-Empirical Meta-Generalized Gradient Approximation Designed for Molecules and Solids. *Phys. Rev. Lett.* **2003**, *91*, 146401.
(60) Dunning, T. H. Gaussian basis sets for use in correlated molecular calculations. I. The atoms boron through neon and hydrogen. *J. Chem. Phys.* **1989**, *90*, 1007−1023.
(61) Clark, T.; Chandrasekhar, J.; Spitznagel, G. W.; Schleyer, P. V. R. Efficient diffuse function-augmented basis sets for anion calculations. III. The 3-21+G basis set for first-row elements, Li-F. *J. Comput. Chem.* **1983**, *4*, 294−301.
(62) Smiga, S.; Fabiano, E.; Laricchia, S.; Constantin, L. A.; Della Sala, F. Subsystem density functional theory with meta-generalized

https://dx.doi.org/10.1021/acs.jpclett.0c02405
J. Phys. Chem. Lett. 2020, 11, 8208−8215

gradient approximation exchange-correlation functionals. *J. Chem. Phys.* **2015**, *142*, 154121.
(63) Śmiga, S.; Fabiano, E.; Constantin, L. A.; Della Sala, F. Laplacian-dependent models of the kinetic energy density: Applications in subsystem density functional theory with meta-generalized gradient approximation functionals. *J. Chem. Phys.* **2017**, *146*, 064105.
(64) Mejía-Rodríguez, D.; Trickey, S. B. Deorbitalization strategies for meta-GGA exchange-correlation functionals. *Phys. Rev. A: At., Mol., Opt. Phys.* **2017**, *96*, 052512.
(65) Mejía-Rodríguez, D.; Trickey, S. B. Meta-GGA Performance in Solids at Almost GGA Cost. *arXiv* 2020, 2008.12420.

https://dx.doi.org/10.1021/acs.jpclett.0c02405
J. Phys. Chem. Lett. 2020, 11, 8208−8215